Journal of Physics and Chemistry of Solids 71 (2010) 1629–1633

Contents lists available at ScienceDirect

Journal of Physics and Chemistry of Solids

journal homepage: www.elsevier.com/locate/jpcs

Properties of In_2S_3 thin films deposited onto ITO/glass substrates by chemical bath deposition

B. Asenjo [a,*], C. Guillén [a], A.M. Chaparro [a], E. Saucedo [b], V. Bermudez [b], D. Lincot [b], J. Herrero [a], M.T. Gutiérrez [a]

[a] Department of Energy, CIEMAT, Avda. Complutense, 22, 28040 Madrid, Spain
[b] Institute of Research and Development of Photovoltaic Energy (IRDEP-UMR 7174-CNRS-EDF-ENSCP), 6 quai Watier, 78401 Paris, France

ARTICLE INFO

Article history:
Received 24 March 2009
Received in revised form
7 September 2010
Accepted 14 September 2010

Keywords:
A. Thin films
B. Chemical synthesis
C. Raman spectroscopy

ABSTRACT

In_2S_3 films have been chemically deposited on ITO coated glass substrates by chemical bath deposition, using different deposition times and precursor concentrations. The bilayers are intended for photovoltaic applications. Different characterization methods have been employed: optical properties of the films were investigated from transmittance measurements, structural properties by XRD and micro-Raman, and surface morphology by SEM microscopy analysis. Also, the direct and indirect band-gaps and the surface gap states were studied with surface photovoltage spectroscopy (SPS). We proposed that electronic properties of the In_2S_3 samples are controlled by two features: shallow tail states and a broad band centred at 1.5 eV approximately. Their relation with the structure is discussed, suggesting that their origin is related to defects created on the S sub-lattice, and then both defects are intrinsic to the material.

1. Introduction

Indium sulphide buffer layers, prepared by chemical bath deposition (CBD), have demonstrated their potential to obtain high efficiency solar cells [1,2]; their band gap energy values of between 2 and 3.7 eV [3], their transparency, etc., are suitable characteristics for application in solar energy conversion. For obtaining In_2S_3 with the adequate properties for such application, we must take into account several considerations about the material.

These properties of In_2S_3 obtained by the CBD method depend on different factors such as precursor concentration, deposition time and reaction temperature. However, the effect of the different conditions on the final layer properties is still not well understood and is one of the key points for the further development of this material. In particular for example, the presence of surface states is very important because of their effect on junction formation in solar cells; hence, it is mandatory to know their origin and properties [4]. Commonly, this type of surface defects is possibly due to recombination centres, which strongly deteriorate the interface between the absorber and the buffer layers, and as a consequence the final device performance.

In this work, a combination of optical, morphological and structural characterization is used to explore the In_2S_3 layers, together with surface photovoltage spectroscopy (SPS), in order to characterize the surface defect structure. Attention is mostly concentrated to study the effect of the different growth conditions on the formation, origin (intrinsic, extrinsic) and properties of the surface states, and their possible impact on the electronic properties of the buffer layer. Samples were prepared using different precursor concentrations and growth times with the aim of identifying the effect of both parameters.

2. Experimental

ITO thin films have been prepared by rf magnetron sputtering from an oxide ceramic target 90 wt% In_2O_3 and 10 wt% SnO_2. The substrates were soda lime glasses (2 mm thick) that were placed in equivalent positions in an adjustable vertical frame and moved in front of the target to obtain simultaneous ITO deposition, without intentional heating. High purity Ar and O_2 were introduced through independent mass flow controllers after the vacuum chamber was evacuated below 1×10^{-4} Pa. The oxygen content in the sputter gas, as determined by the oxygen to argon partial pressure ratio, was adjusted in order to optimize the ITO properties according to previous studies [5,6]. The process total pressure was kept at 4×10^{-1} Pa and the sputtering power density employed was below 1.5 W/cm^2. The samples were later annealed at 350 °C in vacuum in order to improve their optical and electrical characteristics [7], achieving visible transmittance

* Corresponding author. Tel.: +34 913466364; fax: +34 913466037.
E-mail address: mbegona.asenjo@ciemat.es (B. Asenjo).

0022-3697/$ - see front matter © 2010 Elsevier Ltd. All rights reserved.
doi:10.1016/j.jpcs.2010.09.011

Table 1
In_2S_3 films prepared on glass/ITO substrate.

Sample	[TA] (M)	Deposition time (min)	Thickness (nm)
F1	0.3	25	55
F2	0.3	35	70
F3	0.5	25	80
F4	0.5	35	85

Other growth conditions: 70 °C bath temperature, $InCl_3$, 0.01 M HCl, 0.3 M CH_3COOH.

near 90% and sheet resistance of 7 Ω/sq for the present ITO layers with about 350 nm thickness.

The deposition of In_2S_3 was carried from an acidic solution of thioacetamide concentration (TA) (CH_3CSNH_3, Fluka), and indium (III) chloride ($InCl_3$, Fluka) 0.01 M at 70 °C, for different deposition times (Table 1). Other additives necessary to obtain films with photovoltaic quality are hydrochloric acid and acetic acid. Some of the samples were annealed at 200 °C in a tubular furnace under flowing nitrogen.

The thickness of the In_2S_3 films obtained was found using a profilometer (Dektak 3030).

Raman microprobe measurements were made on In_2S_3 layers before and after thermal treatment using a HR800-UV Horiba-Jobin Yvon spectrometer coupled with an Olympus metallographic microscope. The spectra were obtained using as excitation the green line of an Ar+ laser ($\lambda=514$ nm) and were fitted using the LabSpec software defining the peaks as Gaussian–Lorentzian.

Surface photovoltage spectroscopy (SPS) was carried out using a home-made equipment consisting in an isolated camera with a gold grid (Kelvin probe S, Besocke Delta Phi GmbH), controlled by a Kelvin Control 07. Ar pressure of 1 atm was imposed and the measurements were carried out at room temperature. Excitation was made with the light of a monochromator Spectra Pro 2300i 0.3 m (350–1400 nm) with an ARC Model TS-428 250 W Tungsten-Halogen lamp. The surface photovoltage signal was monitored with an oscilloscope Iso-Tech ISR635 35 MHz and measured with a Keithley 2010 Multimeter. The collected signal was corrected using the dark contact potential difference (CPDD) and the wavelength dependence of the lamp emission spectra, on the studied energy region. The indirect and direct band-gaps and the energy of the exponential defect tails were obtained using analysis of the SPS spectra.

Optical transmission measurements of the samples referred to the air were carried out with unpolarised light at normal incidence in the wavelength range from 300 to 2500 nm, with a double beam spectrophotometer Perkin Elmer lambda 9.

X-ray diffraction (Philips X'pert-MPD diffractometer) was used to determine the crystallographic structure of the films; phase identification was carried out by comparing the observed d-spacing with the powder diffraction standards card files and SEM microscopic analysis (Hitachi S-2500) to study the surface morphology.

3. Results and discussion

The optical transmittance spectra corresponding to the different indium sulfide films are shown in Fig. 1. The transmittance of samples (Fig. 1a) in the visible spectral range (400–800 nm) is above 70–80%, with the transmittance being lower for films with high time deposition (and then thicker), whereas transmittance in the near-infrared region decreases owing to interaction with free-carriers in the ITO coating [5–7],

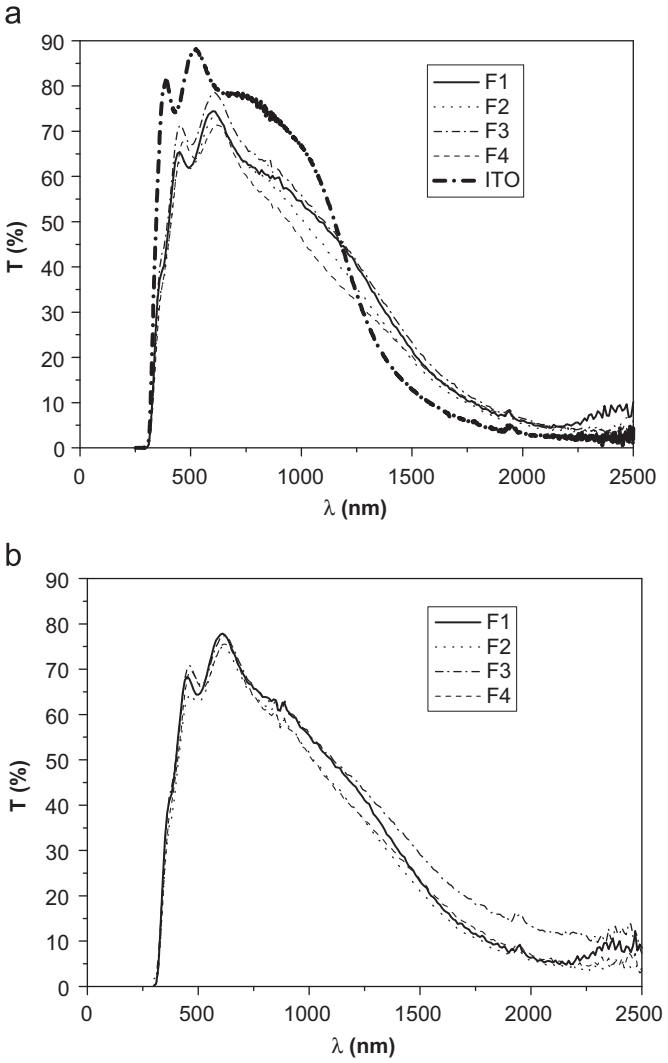

Fig. 1. Optical transmittance spectra for indium sulfide films on ITO/glass substrates (a) and (b) after the thermal treatment at 200 °C under nitrogen atmosphere.

suggesting the presence of high shallow state density as will be confirmed later by SPS.

The X-ray diffractograms corresponding to the samples are shown in Fig. 2. The In_2S_3/ITO films were annealed at 200 °C in nitrogen atmosphere due to the low crystallinity exhibited by the In_2S_3 films. The diffraction peaks of 2θ associated with ITO are at 21.5°, 30.5°, 35.5°, 41.7°, 45.7°, 50.7°, 60.6°, 62.0° and 63.6° (JCPDS Card no. 06-0416) corresponding to a cubic structure with (2 2 2) preferential orientation. The diffraction peaks of 2θ at 33.10°, 43.6° and 47.6° corresponding to In_2S_3 (JCPDS Card no. 32-0456) appear with small intensity in the F1, F2 and F4 samples. This is not surprising because of the very low sample thickness, their nanocrystalline structure and their poor quality.

The optical transmittance spectra corresponding to these samples (Fig. 1b) show an increase in transmittance between 5% and 10% in the range 400–800 nm, the transmittance being lower for films with high time deposition, as the samples without heat treatment.

The Raman spectra of as-grown In_2S_3 are shown in Fig. 3a for samples F1–F4. Raman modes are observed in the energy region between 200 and 500 cm^{-1}, but all of them are broad and have very low intensity, confirming the nanocrystalline or amorphous nature of these samples. Bands observed between 200 and 400 cm^{-1} can be assigned to β-In_2S_3 [8,9], but the band at

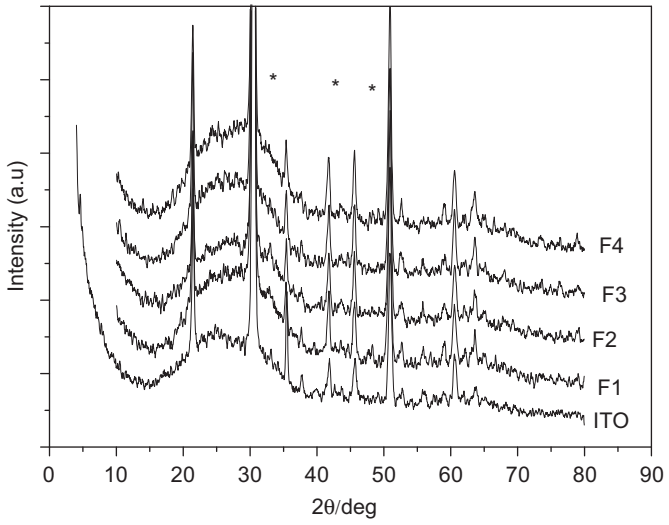

Fig. 2. XRD of samples F1–F4 after the thermal treatment at 200 °C under nitrogen atmosphere (*=corresponding In_2S_3 CJCPDS Card no. 32-0456).

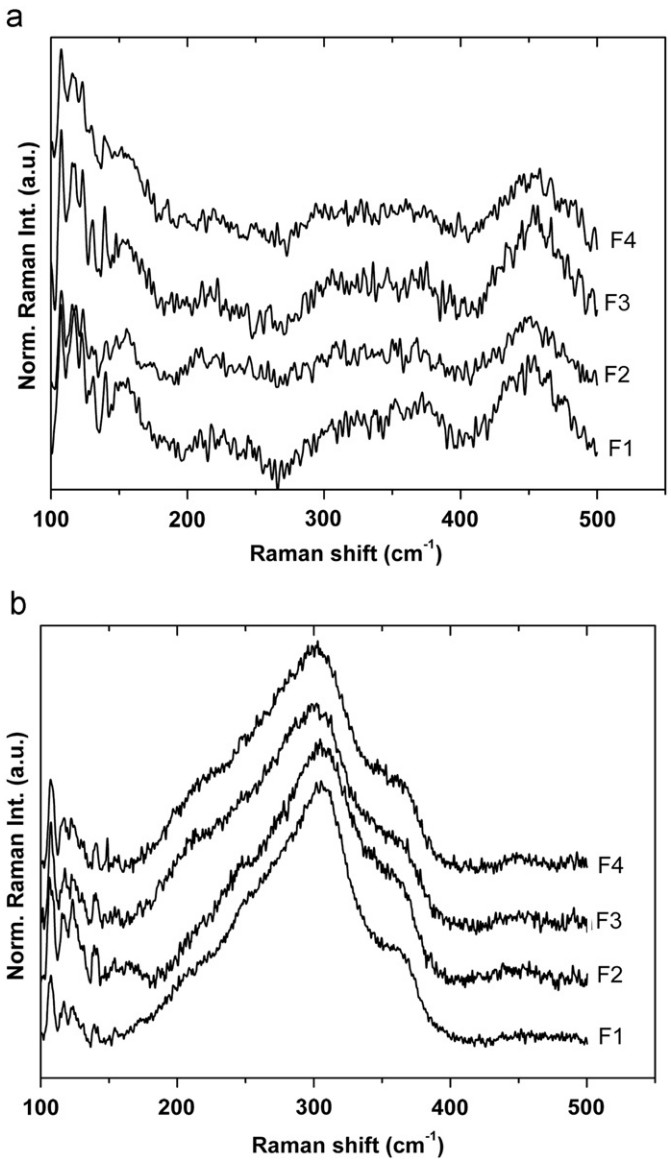

Fig. 3. Raman spectra of samples F1–F4 before (a) and after (b) the thermal treatment at 200 °C under nitrogen atmosphere.

460 cm^{-1} could be related to the S–S mode of elemental S [10], an indication being that free S is present in the samples. From Fig. 3a it is evident that, the lower the growth time (F1 and F3), the higher the intensity of the band at 460 cm^{-1}, suggesting that for higher growth times there is a lack of S in the bath. After the thermal treatment at 200 °C, spectra change as is clearly observed in Fig. 3b. The band at 460 cm^{-1} assigned to the S–S vibrational mode of elemental S almost disappears, presumably due to S evaporation and/or reaction with the as-grown layers, suggesting that many free S atoms cannot form the In–S bonds before the thermal treatment. Also, several peaks and bands are enhanced in the whole frequency region. The active modes of β-In_2S_3 are present at 105, 117, 250, 305 and 363 cm^{-1} [7,8], confirming the composition and structure of the layers. Their nanocrystalline or quasi-amorphous nature is reflected in the broadening of the bands (mostly in the high frequency bands), indicating that although some crystallization occurs after thermal treatment, the layers still remain polycrystallines and/or nanocrystallines, making an in-deepth study of the spectra difficult. In any case, the Raman bands do not show any tendence, either with deposition time or with bath concentration. This means that both conditions seem not to affect considerably the sample's structure after the thermal treatment (almost at large scale), the active Raman modes corresponding to the β-In_2S_3 phase being present in all the cases.

Concerning the SPS measurements, the first important point is that all the samples have n-type conductivity as was expected. In Fig. 4a the squared (W-CPD) difference is plotted for the as-grown samples, where *W* is the maximum contact potential that is obtained at high energies (the value was taken nominally at 3.5 eV in all the cases) and CPD is the contact potential difference [11,12]. Note that before the thermal treatment, the surface photovoltage signal is very low. Hence, it is not possible to accurately determine the direct and indirect band-gaps and then, these spectra will be only qualitatively discussed taking into account two important features: the broad onset at high energies and the broad band centred at 1.5 eV approximately. The broad onset can be attributed to the presence of shallow states, extending from their corresponding band up to the band-gap (tail states) [11]. In such a case, there is a high density of shallow states in the samples (especially in the samples grown from low concentration solutions), in agreement with their poor crystallinity confirmed by XRD and Raman spectroscopy. Observing Fig. 4a, it is possible to establish two important correlations: the lower the concentration and growth time, the higher the broad onset. In any case, the bath concentration seems to affect more than the growth time. Similar to the as-grown samples, this band could be related to the first growth steps where surface instabilities are largely expected, due to unsatisfied bonds, for example. Further growth steps lead to a lower density of tail states on the surface, probably because the last growth steps are under a more stable regimen.

In addition, when the growth time exceeds 25 min and/or the precursor concentration 0.3 M, a broad band centred at 1.5 eV starts to dominate the spectra. There are few reports on defect levels on In_2S_3 in general and about this energy region in particular [13], but with a simple reasoning we can try to obtain more information on it. The material being n-type (holes are minority carriers), the increase in photovoltage implies the generation of minority carriers, i.e. holes. Then, in the spectra of Fig. 4a at 1.5 eV we can observe the excitation of holes from a hole-trap centre (probably positively charged and with donor character), in agreement with the observation in Ref. [13]. Although it is not possible to establish the actual origin of this centre, their hole-trap properties could be related for example

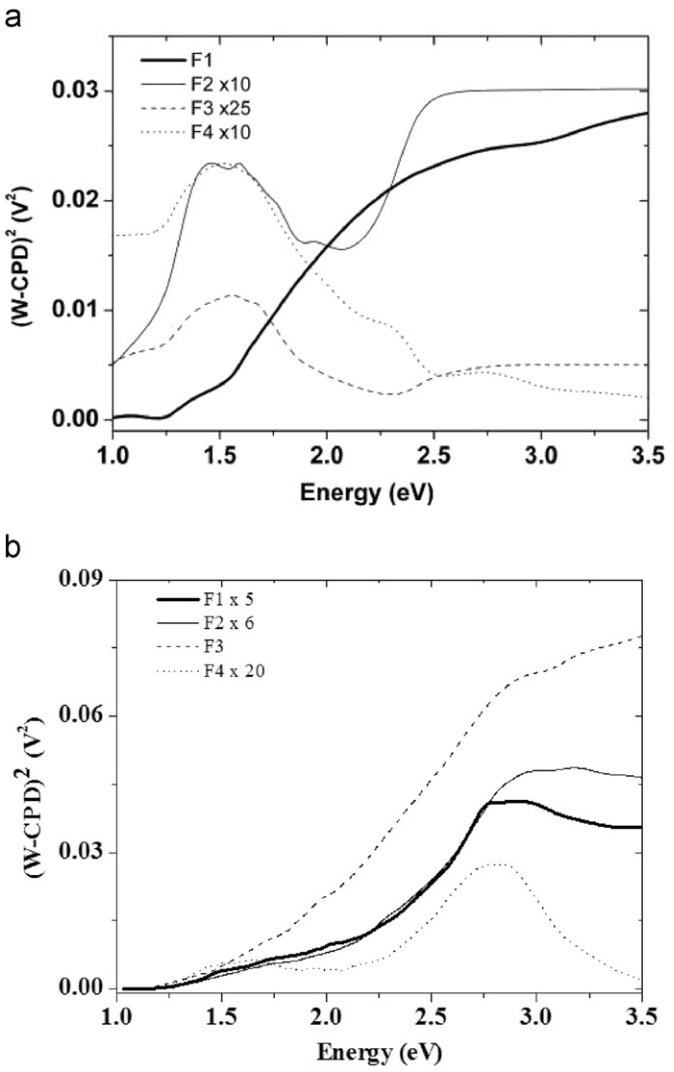

Fig. 4. SPS spectra of samples F1–F4 before (a) and after (b) the thermal treatment at 200 °C under nitrogen atmosphere.

with positive charged centres, formed by anion vacancy in the In_2S_3 lattice: V_S (the charge of the centre could be +1 or +2, in agreement with their hole-trap properties). This is also in agreement with the Raman measurements, where free S was observed, indicating that some S atoms were not included on the In_2S_3 structure, the origin being the V_S and also with the conductivity type of samples, because this intrinsic defect (V_S) can explain n-type conductivity. This band seems to be more dependent on growth time.

After the thermal treatment the surface photovoltage spectra dramatically change as is clearly observed in Fig. 4b. The photovoltage markedly increases and the SPS spectra exhibit a well defined band edge. In order to analyse the spectra, numerical fitting using sigmoidal logistic functions was employed. Means these fittings we obtain both band gaps which are summarized in Table 2. Also, with the slope of the plot of the difference (W-CPD) as a function of the photon excitation energy in semi-log scale, we obtain the exponential defect tails below the band-gap (E_t), or Urbach-energy, which is directly related to the disorder on the surface [12], and is also summarized in Table 2.

The results are in agreement with the reported values for In_2S_3 layers [14–17] and, as can be observed in Table 2, the direct band-gap tends to decrease with bath concentration. No special correlations of the indirect band-gap are observed, either with

Table 2
Summary of the values extracted from SPS measurements (room temperature) of samples with the thermal treatment at 200 °C under nitrogen atmosphere.

Sample	E_g dir. (eV)	E_g ind. (eV)	E_t (meV)
F1	2.57 ± 0.01	1.69 ± 0.06	61 ± 2
F2	2.61 ± 0.01	1.75 ± 0.10	69 ± 1
F3	2.51 ± 0.02	1.77 ± 0.05	141 ± 2
F4	2.48 ± 0.03	—	42 ± 1

the bath concentration or with the growth time. It is evident that samples F1 and F2 present similar spectra and although the signal is considerably improved after heating, the presence of the band onset is also clear. Both samples being grown at low bath concentration, this is an indication that the deposition regime in the two cases was the same. Conversely, sample F3 strongly increases its signal after crystallization and is very different from that of sample F4. It is worthnoticing that shallow states for sample F3 are the major contribution factor to the photovoltage at high energies, indicating a disordered system in agreement with the XRD spectrum. To explain this phenomenon, we can take into account the growth conditions. At higher bath concentration, the first steps on the growth occur at high deposition rates (as is the case of sample F3), and the layer gets a low crystalline quality. After a certain point of time, the bath concentration decreases and the growth rate starts to decrease, explaining the better crystalline quality of the sample F4. In fact, the sample F4 behaves differently from others as is clearly observed in Fig. 4b. The broad onset diminishes and almost disappears, implying the minimization of the tail states density [11], and is accompaigned by a low signal.

These tendencies are confirmed by the value of the Urbach-energy (E_t) presented in Table 2. While samples F1 and F2 are comparable, the value of E_t for sample F3 is considerably higher and for F4 it is considerably lower. In such a case, the disorder on the systems is related to the shallow surface states (tail states) and as a consequence the lower the Urbach-energy, the lower the band onset. Finally, the broad band centred at 1.5 eV for the precursors strongly decreases and shifts to higher energies after thermal treatment. The rearrangement of the atoms after the thermal process can explain this behaviour and it seems to be effective in eliminating this undesirable band absorption, probably for the diffusion of S in order to compensate the V_S.

SEM images (Fig. 5) show the surface morphology of the films. For the F1 layer the surface is very compact and homogeneous microstructure compared with the other samples, but all of the samples show nanocrystalline structure as is expected, with grain sizes lower than 100 nm.

4. Conclusions

β-In_2S_3 layers were prepared by the CBD method with nanocrystalline and/or amorphous structure, as confirmed by XRD and Raman spectroscopy. As-grown samples exhibit poor crystalline quality with free S as the main secondary phase. The crystalline quality of the layers is enhanced after thermal treatment at 200 °C, as observed from the elimination of the free S by evaporation and/or diffusion onto the layer. The surface photovoltage spectra of as-grown CBD In_2S_3 shows two distinct features: a broad onset at high energies related to the tail states and a broad band at 1.5 eV with donor character and presumably related to anion vacancies. The contribution of both bands to the total surface photovoltage depends on the growth conditions, which seems to be responsible for the control of the optical and electrical properties of the layers. With a bath concentration of 0.5 M and a growth time of 35 min and after the crystallization process at 200 °C (sample F4), the surface tail

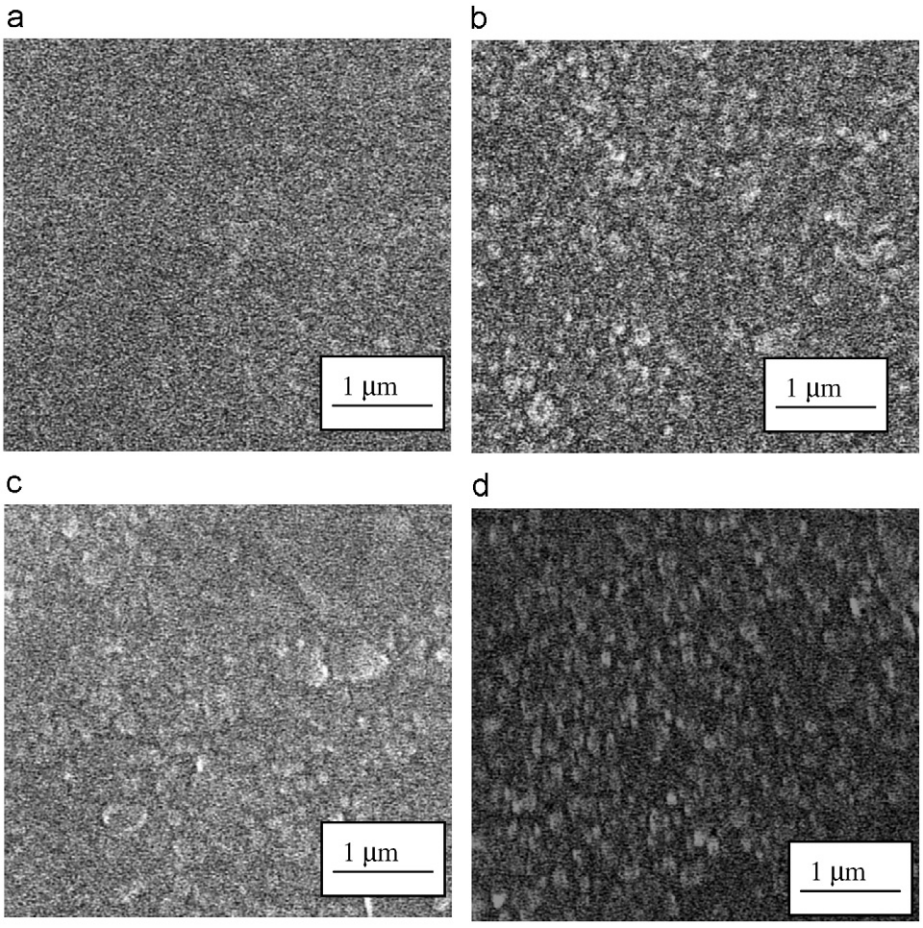

Fig. 5. SEM images of In_2S_3 films: F1 (a), F2 (b), F3 (c) and F4 (c) deposited at 70 °C on glass and annealing at 200 °C under nitrogen atmosphere.

states are minimized and the Urbach-energy is also considerably reduced, obtaining In_2S_3 layers with electronic and structural properties suitable for their application as buffer layers in photovoltaic devices. Unfortunately, the transparency of the film is reduced due to their thicker nature at undesirable values. Future works will be focused on the optimization of the optical parameters without deterioration of the electronic and structural ones.

Acknowledgements

This work has been financed by the FOTOFLEX project (Comunidad de Madrid) and "Células fotovoltaicas ligeras y flexibles" by Fundación Ramón Areces.

References

[1] N. Naghavi, S. Spiering, M. Powalla, B. Canava, D. Lincot, Prog. Photovolt.: Res. Appl. 11 (2003) 437.
[2] S. Spiering, A. Eicke, D. Hariskos, M. Powala, N. Naghavi, D. Lincot, Thin Solid Films 451–452 (2004) 562.
[3] R. Bayón, C. Guillén, M.A. Martínez, M.T. Gutiérrez, J. Herrero, Electrochem. Soc. 145 (1998) 2775.
[4] S. Gall, N. Barreau, S. Harel, J.C. Bernède, J. Kessler, Thin Solid Films 480–481 (2004) 138.
[5] C. Guillén, J. Herrero, Vacuum 80 (2006) 615.
[6] C. Guillén, J. Herrero, J. Appl. Phys. 101 (2007) 073514.
[7] C. Guillén, J. Herrero, Thin Solid Films 510 (2006) 260.
[8] J. Alvarez-Garcia, A. Perez-Rodriguez, A. Romano-Rodriguez, T. Jawhari, J.R. Morante, R. Scheer, W. Calvet, Thin Solid Films 387 (2001) 216.
[9] Y. Xiong, Y. Xie, G. Du, X. Tian, Y. Qian, J. Solid State Chem. 166 (2002) 336.
[10] G. Parker, R. Woods, G. Hope, Colloids Surf. A: Physicochem. Eng. Aspects 318 (2008) 160.
[11] L. Kronik, Y. Shapira, Surf. Sci. Rep. 37 (1999) 1.
[12] J. Mwabora, K. Ellmer, A. Belaidi, J. Rappich, W. Bohne, J. Föhrich, Th. Dittrich, Thin Solid Films 516 (2008) 3841.
[13] A. Timoumi, H. Bouzouita, M. Kanzari, B. Rezig, Thin Solid Films 480–481 (2005) 124.
[14] B. Asenjo, A.M. Chaparro, M.T. Butierrez, J. Herrero, C. Maffiotte, Electrochim. Acta 49 (2004) 737.
[15] N. Naghavi, R. Henriquez, V. Laptev, D. Lincot, Appl. Surf. Sci. 222 (2004) 65.
[16] S. Gorai, A. Datta, S. Chaudhuri, Mater. Lett. 59 (2005) 3050.
[17] R. Yoosuf, M.K. Jayaraj, Sol. Energy Mater. Sol. Cell 89 (2005) 85.